Published in final edited form as:
Int J Radiat Oncol Biol Phys. 2009 July 15; 74(4): 1217–1225. doi:10.1016/j.ijrobp.2009.03.057.

Celastrol potentiates radiation therapy via impairment of DNA damage processing in human prostate cancer

Yao Dai, Ph.D., **Jeffrey T. DeSano**, **Yang Meng, Ph.D.**, **Qing Ji, M.D., Ph.D.**, **Mats Ljungman, Ph.D.**, **Theodore S. Lawrence, M.D., Ph.D.**, and **Liang Xu, M.D., Ph.D.***
Department of Radiation Oncology, Comprehensive Cancer Center, University of Michigan, Ann Arbor, MI 48109

Abstract

Purpose—Celastrol is an active ingredient of traditional herbal medicine and has recently been identified as a potent natural proteasome inhibitor. In this study, we evaluated the radiosensitizing potential of Celastrol in the human prostate cancer PC-3 model.

Materials and Methods—Clonogenic assays were performed to determine the radiosensitizing effect of Celastrol. Apoptosis was examined by flow cytometry using Annexin V and propidium iodide staining and by a caspase-3 activation assay. DNA damage processing was examined by immunofluorescent staining and Western blot for phosphorylated H2AX (γH2AX). PC-3 xenograft model in athymic nude mouse was exployed for *in vivo* efficacy of Celastrol in combination with radiation. The tumor samples were also analyzed for apoptosis and angiogenesis.

Results—Celastrol sensitized PC-3 cells to ionizing radiation (IR) in a dose- and schedule-dependent manner, where pretreatment of Celastrol for 1 h followed by IR achieved maximum radiosensitization. Celastrol significantly prolonged the presence of IR-induced γH2AX and increased IR-induced apoptosis. Celastrol combined with fractionated radiation significantly inhibited PC-3 tumor growth *in vivo* without obvious systemic toxicity. The combination treatment increased γH2AX levels and apoptosis, induced cleavage of poly(ADP-ribose)polymerase (PARP) and Mcl-1, as well as reduced angiogenesis *in vivo*, as compared with either treatment alone.

Conclusions—Celastrol sensitizes PC-3 cells to radiation both *in vitro* and *in vivo*, by impairing DNA damage processing as well as by augmenting apoptosis. Celastrol may represent a promising new adjuvant regime for the treatment of hormone-refractory prostate cancer.

Keywords

Celastrol; radiosensitization; prostate cancer; DNA repair; apoptosis

INTRODUCTION

Radiation therapy is the mainstay in the treatment of locally advanced prostate cancer (1). However, local recurrence and radioresistance still remain significant clinical problems that

*Corresponding Author: Liang Xu, M.D., Ph.D., Department of Radiation Oncology, Division of Cancer Biology, University of Michigan, 4424E Med Sci I, 1301 Catherine St., Ann Arbor, MI 48109-5637, Tel: 734-615-7017, Fax: 734-615-3422, E-mail: liangxu@umich.edu.

Conflict of Interest Notification: None

lead to therapeutic failure (2). Although androgen-ablation therapy combined with radiation have shown beneficial effects on relapse-free time and overall survival, therapy for advanced human prostate cancer is limited by the propensity of the disease to progress from an androgen-dependent to an androgen-independent phenotype. Despite the activation of the cellular apoptotic machinery in androgen-independent prostate cancer cells by ionizing radiation (3), acquired radiation resistance can develop in hormone-refractory prostate cancers that is associated with poor prognosis (4). To overcome primary or acquired radioresistance, rational strategies have been designed to target radiation-induced DNA damage response (DDR) pathways, such as DNA repair, cell cycle checkpoints and apoptosis (5). In previous studies, we have shown that inhibition of anti-apoptotic proteins by specific small molecule inhibitors sensitized prostate cancer cells to radiation therapy potentially by augmenting apoptosis (6, 7).

Proteasome inhibitors are promising candidates for the treatment of human cancers, as proteasomes are responsible for the degradation of various intracellular regulatory proteins that take part in multiple cellular activities including proliferation, survival, cell cycle, and apoptosis (8). Bortezomib (Velcade; PS-341), the first proteasome inhibitor that have had clinical applications, has demonstrated impressive antitumor activity as a single agent in a variety of human malignancies including prostate cancer (9). Bortezomib has been proven to be an effective radiosensitizer in preclinical models of androgen-independent prostate cancer (10). Many other proteasome inhibitors are currently being tested in preclinical models, either alone or in combination with radiotherapy (11). These studies suggest that proteasome inhibition may sensitize tumor cells to radiation, thus providing a strong rational to further investigate proteasome inhibitors as radiosensitizers.

Celastrol is an active ingredient of a traditional Chinese medicine derived from plants of the *Celastreceae* family (12). Celastrol exhibits antiproliferative and apoptosis-inducing effects in tumor cells, revealing a potential use in cancer treatment (13). It was proposed that Celastrol preferentially inhibits the chymotrypsin-like activity of the 26S proteasome, and induces apoptosis in both *in vitro* and *in vivo* prostate cancer models (12). To our knowledge, there are no reports on the use of Celastrol in combination with ionizing radiation for cancer therapy, although a recent study shows that triptolide, a homologue of Celastrol, enhances the radiation response in pancreatic cancer cells (14). In the current study, we determined that Celastrol has efficacy as a radiation sensitizer in both *in vitro* and *in vivo* models of androgen-independent prostate cancer and explored the potential mechanism of Celastrol-mediated radiosensitization.

MATERIALS AND METHODS

Reagents and cell culture

Celastrol (98%) was purchased from Gaia Chemical Corporation (Gaylordsville, CT). The powder was reconstituted in dimethyl sulfoxide (DMSO) and stored as aliquots at −70°C for *in vitro* study. All tissue culture reagents were purchased from Invitrogen (Grand Island, NY). Phospho-specific anti-H2AX (γH2AX) antibodies (JBW301) were obtained from Upstate (Upstate Biotechnology, Lake Placid, NY). Antibodies against poly(ADP-ribose) polymerase (PARP) (F-2), Mcl-1 (S-19), Mcl-1, Ubiquitin (P4D1), Bcl-2 (C-2) and GAPDH (10B8) were purchased from Santa Cruz Biotechnology (Santa Cruz, CA). Anti-XIAP antibodies were purchased from BD Bioscience (San Jose, CA) and anti-β-actin (AC-74) was purchased from Sigma (St. Louis, MO). Fluorescein isothiocyanate (FITC) conjugated rabbit anti-mouse polyclonal antibody was purchased from Pierce (Rockford, IL). All chemicals were purchased from Sigma unless otherwise indicated. The human prostate cancer cell line PC-3 was purchased from The American Type Culture Collection. Cells were maintained in RPMI 1640 supplemented with 10% FBS, 100 U/ml penicillin, and 100 μg/ml streptomycin, and incubated

in a 5% CO_2 humidified incubator at 37°C. Cytotoxicity/apoptosis assays and Western blot were performed as previously described (7,15).

Colony formation and clonogenic survival assay

For the colony formation assay, PC-3 cells were seeded in a 6-well plate and treated with varying concentrations of Celastrol in triplicate. After 12–14 days incubation, plates were gently washed with PBS and stained with crystal violet (0.1% in PBS). Colonies with over 50 cells were manually counted. Plating efficiency was calculated by dividing the number of colonies formed in the treated group by the number formed in the untreated control group. Clonogenic survival assays were carried out after the cells were treated with Celastrol and radiation according to the indicated schedules and the enhancement ratio (ER) of the Celastrol treatment was calculated as previously described (7),

Immunofluorescence

Cells cultured on a chamber slide (Lab-Tek) were washed once with PBS and then fixed in 2% formaldehyde in PBS for 15 min at room temperature. Cells were permeabilized and blocked with blocking buffer (5% normal goat serum, 0.2% Triton X-100 in PBS) for 1 h and incubated with antiγH2AX monoclonal antibody (1:1000 in block buffer) for 1 h at room temperature. After washing with PBS 3 times, cells were incubated with FITC-labeled rabbit anti-mouse antibody (1:200 in blocking buffer) for 1 h and washed with PBS 3 times. Nuclei were counterstained with 4′,6′-diamidino-2-phenylindole (DAPI) (10 μg/ml in PBS) for 10 min before cells were covered by anti-fade solution (Fisher) and mounted. Immunofluorescence was observed at a 400-fold magnification with a live fluorescence microscope (Olympus).

Animal studies

Female athymic NCr-nu/nu mice (5~6 weeks) were inoculated subcutaneously (s.c.) on both sides of the lower back above the tail with 3×10^6 cells/0.2 ml of PC-3 cells. When tumors reached a size of about 100 mm^3, the mice were randomized into 4 groups with 8~10 mice per group and they were treated daily with (*a*) vehicle control [10% DMSO, 70% Cremophor/ethanol (3:1, v/v) and 20% PBS] (12); (*b*) Celastrol at a dose of 1 mg/kg; (*c*) X-ray radiation at 2 Gy fraction/day, as described previously (6); or (*d*) X-ray radiation at 2 Gy fraction/day, plus Celastrol (1 mg/kg). Celastrol or vehicle control buffers were injected intraperitoneally (*i.p.*) 5 days/week for 3 weeks (q.d.5 × 3), and radiation was performed 5 days/week for 2 weeks (q.d.5 × 2). In Group (d), Celastrol was injected 1 h before irradiation. Tumor size and body weight were measured twice a week. Tumor volumes were calculated using the formula: (length × $width^2$)/2. After the last dose of Celastrol (day 18), tumor growth inhibition (T/C %) of each treatment group was calculated, and tumors from one mouse in each group were collected for protein and histological analysis. For histological detection, tumor samples were paraffin embedded by fixation in 4% paraformaldehyde at 4°C overnight. Besides hematoxylin and eosin (H&E) staining, histological sections were subjected to Terminal deoxynucleotidyl Transferase Biotin-dUTP Nick End Labeling (TUNEL) staining using an *in situ* ApopTag kit for apoptosis detection. Tumor angiogenesis was analyzed by anti-mouse CD31 staining (15). Both TUNEL and CD31 positive cells were quantified by a blinded observer. Throughout the experiment, tumor doubling time was evaluated by determining the first day when the tumor volume was twice the baseline volume, and characterized by Kaplan-Meier estimate (16). All experiments were performed according to protocols approved by the University of Michigan Committee for Use and Care of Animals.

Statistical analysis

The two-tailed Student's *t*-test and the two-way ANOVA analysis were employed and the cell and animal data were presented using GraphPad Prism 5.0. A threshold of $p < 0.05$ was defined as statistically significant.

RESULTS

Celastrol enhances IR-induced cytotoxicity

To determine the cytotoxicity of Celastrol combined with IR, PC-3 cells were treated with two different concentrations of Celastrol (0.2 and 0.4 μM) together with different doses of irradiation. It was found that at the concentration of 0.4 μM, but not 0.2 μM, Celastrol sensitized the PC-3 cells significantly to IR ($p<0.01$ at 2 Gy; $p<0.001$ at 4 and 6 Gy) (Fig. 1*A*). In the clonogenic survival assay, at concentrations that minimally affected plating efficiency (~90% for 0.2 μM and ~70% for 0.4 μM, respectively) (Fig. 1*B*), Celastrol dose-dependently enhanced IR-induced clonogenic cell killing ($p< 0.01$) (Fig. 1*C*). Celastrol achieved enhancement ratio (ER) of 1.18±0.02 and 1.38±0.06 at concentrations of 0.2 μM and 0.4 μM, respectively. These results show that Celastrol potently sensitizes PC-3 cells to IR.

Radiosensitization of Celastrol is schedule-dependent

To investigate whether drug-mediated radiosensitization may be treatment regimen-dependent, and to optimize the treatment schedule for the radiosensitizing effect of Celastrol, we treated PC-3 cells with Celastrol and IR using three different schedules (Fig. 1*D*). Although there was a modest radiosensitization (ER= 1.21 ± 0.05) when cells were pre-incubated with Celastrol for 24 h before irradiation (*Schedule I*), pretreatment of Celastrol for 1 h followed by irradiation (*Schedule II*) achieved substantially higher enhancement ratio (ER= 1.42 ± 0.03) (Fig. 1*D*). Incubation of Celastrol for 24 h both before and after irradiation (*Schedule III*) resulted in an enhancement ratio of 1.33 ± 0.07 (Fig. 1*D*). These data clearly show the importance of treatment scheduling for optimal therapeutic outcome and suggest that *Schedule II* is the optimal treatment schedule of the three schedules tested. This scheduling was therefore selected for all subsequent experiments.

Celastrol impairs IR-induced DNA damage processing

Interference with radiation-induced DNA damage repair pathways is one of the major mechanisms involved in radiosensitization (17). To explore the effect of Celastrol on IR-induced DNA damage processing, we investigated the kinetics of appearance and disappearance of phosphorylated histone H2AX (γH2AX), an indicator of DNA damage and DNA damage processing (18–20). Kinetic analysis showed that Celastrol significantly increased the level of radiation-induced γH2AX versus untreated control ($p< 0.01$) and this was correlated with an increase of ubiquitylated proteins (Fig. 2*A*, *B*). Since repair of radiation-induced double strand breaks leads to the reversal of phosphorylation of H2AX, our finding that Celastrol delayed γH2AX reversal suggests that Celastrol may slow DNA double-strand break repair. Consistent with such hypothesis are the results obtained by immunocytochemistry showing that radiation-induced γH2AX foci remained significantly longer in the presence of Celastrol treatment than untreated control ($p<0.001$, Fig. 2*C*, *D*). Taken together, these results suggest that Celastrol inhibits IR-induced DNA double-strand break repair.

Celastrol promotes IR-induced apoptosis

Apoptosis is a minor but important mode of cell death induced by ionizing radiation (21). We found that after 72 h of combination treatment, cells had undergone more apoptosis than following either treatment alone (Fig. 3*A*), as evidenced by caspase-3 activation (Fig. 3*B;* $p<0.05$ *vs*. IR alone; $p<0.01$ *vs*. Cel alone) and cleavage of the caspase substrates PARP and

Mcl-1 (Fig. 3*C*). Addition of the caspase inhibitor zVAD reduced apoptosis (Fig. 3*A*), caspase-3 activity (Fig. 3*B; p*<0.01) and PARP and Mcl-1 cleavage (Fig. 3*C*) induced by Celastrol combined with IR. These results suggest that the sensitizing effect of Celastrol may involve augmentation of radiation-induced apoptosis.

Celastrol sensitizes PC-3 xenografts to ionizing radiation

To evaluate the radiosensitization potential of Celastrol *in vivo*, we employed a PC-3 xenograft tumor model as previously described (6). As shown in Fig. 4*A*, although Celastrol alone exhibited a minor tumor growth inhibitory effect, the combination of Celastrol with IR significantly suppressed tumor growth compared with IR alone ($p<0.01$). By the last day of Celastrol administration (Day 18), median tumor volume by the combination treatment resulted in a 40% tumor regression compared to IR alone ($p<0.001$), and an 80% tumor regression compared to the untreated control (Table 1). We found that the combination of Celastrol with radiotherapy significantly increased the tumor doubling time (growth retardation) compared with radiotherapy alone (Fig. 4*B*). The median tumor doubling time increased from 5.5 days in control tumors to 6.0 days in irradiated tumors and to 25 days for tumors treated with the combination of Celastrol and IR (Table I). It is important to note that the mice tolerated the combination therapy well, with only modest weight loss that was reversed quickly after the completion of treatment (Fig. 4*C*). These results demonstrate that the dose-schedule of Celastrol that significantly radiosensitized prostate cancer *in vivo* is well tolerated by the mice.

Celastrol enhances IR-induced apoptosis and reduces angiogenesis in vivo

The above *in vitro* data suggest that Celastrol interferes with DNA double-strand break repair and enhances the induction of apoptosis following exposure to IR. To determine whether apoptosis can also be observed *in vivo*, tumors were collected on the last day of drug dosing (Day 18) and were processed for histological examination of apoptosis using TUNEL staining. It was found that the combination treatment resulted in more TUNEL-positive tumor cells than either treatment alone (Fig. 5*A*). When the positively stained cells were quantified in IR alone and combination groups, TUNEL-positive cells increased from (5.8±1.1)/field to (10.5±1.2)/field ($p<0.05$) (Fig. 5*B*), Similar significant difference was observed between Celastrol alone and combination groups ($p<0.05$ for TUNEL, Fig. 5*B*). It was further shown that apoptosis induced by the combination therapy involved significant cleavage of both PARP and Mcl-1 (Fig. 5*D*), indicating caspase activation that was consistent with *in vitro* data (Fig. 3). Moreover, a significant increase of γH2AX was only observed following the combination treatment (Fig. 5*D*), which is probably a reflection of the increased occurrence of apoptosis in the tumor tissue *in vivo*. Combination treatment also showed significantly reduced CD31-positive endothelial cells than either treatment alone (Fig. 5*A*, *C*). It is worth noting that treatment with either Celastrol or IR alone at these doses showed significantly higher levels of apoptosis and less angiogenesis than mock-treated mice ($p<0.05$, Fig. 5*B*, *C*). These *in vivo* data demonstrate that Celastrol augments radiation-induced apoptosis and reduces angiogenesis in human prostate xenografts in mice.

DISCUSSION

In this study, we demonstrate for the first time that Celastrol sensitizes human prostate cancer PC-3 cells to radiation both *in vitro* and *in vivo* in nude mouse xenograft model. The mechanism of sensitization may involve three processes critical for tumor growth and resistance to radiation therapy. *First*, Celastrol appears to impair the processing of DNA damage, as assessed by γH2AX. *Second*, Celastrol significantly augmented radiation-induced apoptosis, which may be a result of the inhibition of DNA repair. *Third*, using anti-CD31 antibodies to stain for blood vessel formation, we found that Celastrol attenuated angiogenesis in prostate cancer xenografts

in nude mice. These results suggest that the natural proteasome inhibitor Celastrol may function as a potent radiosensitizer and abrogate angiogenesis in androgen-independent prostate cancer.

Although our studies suggest that γH2AX removal is associated with increased radiation sensitivity after Celastrol treatment, the mechanism of the interference is not yet fully understood. It is possible that Celastrol interferes with the processing and repair of radiation-induced DNA double-strand breaks. Alternatively, Celastrol may interfere with a post-repair step involving the actual reversal of γH2AX, such as dephosphorylation or degradation and/or a histone exchange of γH2AX (22). However, the role of Celastrol as a radiosensitizer would favor the DNA repair-inhibitory mechanism rather than a general effect on phosphatases or H2AX degradation/exchange. Indeed, our finding is consistent with a report showing that bortezomib downregulates IR-induced DNA damage repair (23). Furthermore, the proteasome inhibitors MG132 and β-lactacystin have been shown to disrupt homologous recombination (HR)-mediated DNA repair induced by γ–irradiation (24). The results from these studies provide support for a model where proteasome inhibition abrogates DNA repair (25). Whether the degradation of γH2AX is mediated by ubiquitin-proteasome pathway remains to be tested. One explanation would be that, H2AX can become polyubiquitylated thus be stabilized by proteasome inhibition, as previously suggested (26).

The delayed kinetics of IR-induced γH2AX in the presence of Celastrol correlates with a reduced survival in the clonogenic survival assay. Using different schedules, a modest radiosensitization was observed by 24 h-pretreatment of Celastrol (*Schedule I*, Fig. 1*D*). This sensitization may be related to a Celastrol-induced G_2/M arrest (data not shown), since cells that are accumulated at the G_2/M border are generally more sensitive to IR (27). However, the radiosensitizing effect of Celastrol was markedly improved with the schedule of 1 h-pretreatment with Celastrol (*Schedule II*), a time when the drug is expected to have entered the cells but not yet had time to alter cell cycle distribution. Unexpectedly, treatment with Celastrol both before and after irradiation (*Schedule III*) did not further improve radiosensitization compared to *Schedule II*. Overall, these results suggest that the radiosensitizing potential of Celastrol is achieved predominantly with the schedule that correlates with depressed DNA damage processing, rather than altered cell cycle distribution.

Apoptosis is regulated by many factors. Efficient processing and repair of DNA damage are major contributors to the suppression of apoptosis as well as clonogenic cell death following genomic insult by radiation or other DNA damage-inducing agents. Thus, any agent that interferes with DNA repair would be expected to potentiate the induction of clonogenic cell death and apoptosis following DNA damage induction. Interestingly, when using the concentrations of Celastrol that did not sensitize cells to radiation-induced apoptosis, we still observed radiosensitization using the clonogenic survival assay. Moreover, blocking caspases using the pan-caspase inhibitor zVAD did not reverse clonogenic cell death by Celastrol (data not shown). In fact, Celastrol-enhanced apoptosis occurred at a relatively late stage after irradiation (72 h), which may be the result of failed DNA repair rather than a direct activation of signals leading to apoptosis. Thus, our results suggest that the radiosensitizing effect of Celastrol observed using the clonogenic survival assay may not be related to a reduced apoptotic threshold. These findings are consistent with a previous report showing that the radiosensitizing effects of the proteasome inhibitor MG132 did not correlate to an increased induction of apoptosis in PC-3 cells (28).

Our *in vivo* PC-3 xenograft model showed a marked enhancement of growth suppression when Celastrol was combined with IR compared to IR alone. Furthermore, Celastrol significantly reduced CD31 staining for microvessel formation in the xenograft model, suggesting that Celastrol alone or combined with radiation has anti-angiogenic activity. Intriguingly, we found that Celastrol treatment significantly augmented radiation-induced apoptosis in the tumor

tissue as measured with the TUNEL assay and γH2AX expression. Thus, although apoptosis does not appear to play an important role in clonogenic survival *in vitro*, it may contribute to the radiosensitizing effect of Celastrol *in vivo*.

Taken together, our study demonstrates that Celastrol is a potent radiosensitizer both *in vitro* and *in vivo.* The mechanism of this sensitization may involve the abrogation of DNA repair which in turn may explain the increased loss of clonogenic survival, augmentation of radiation-induced apoptosis and the loss of endothelial cells making up the microvasculature. The multiple effects of the natural medicine Celastrol in regulating the radiation response and the tumor microenvironment may provide novel opportunities for the treatment of malignant diseases.

Acknowledgments

Grant support: This study was supported in part by Department of Defense Prostate Cancer Research Program W81XWH-06-1-0010 (to L. X.), NIH R01 CA121830-01 and R21 CA128220-01 (to L. X.), and NIH through a University of Michigan Cancer Center Support Grant (5 P30 CA46592). J. D. is a University of Michigan Undergraduate Research Opportunity Program (UROP) student.

We wish to thank Dr. Susan Harris for help with the manuscript; the University of Michigan Comprehensive Cancer Center (UMCCC) Histology Core for the immunohistology study; UMCCC Unit of Laboratory Animal Medicine (ULAM) for help with animal experiments, and the UMCCC Flow Cytometry Core for flow cytometry analysis.

References

1. Denmeade SR, Isaacs JT. A history of prostate cancer treatment. Nat Rev Cancer 2002;2:389–396. [PubMed: 12044015]
2. Hanks GE, Hanlon AL, Hudes G, et al. Patterns-of-failure analysis of patients with high pretreatment prostate-specific antigen levels treated by radiation therapy: the need for improved systemic and locoregional treatment. J Clin Oncol 1996;14:1093–1097. [PubMed: 8648362]
3. Palayoor ST, Bump EA, Teicher BA, et al. Apoptosis and clonogenic cell death in PC3 human prostate cancer cells after treatment with gamma radiation and suramin. Radiation Research 1997;148:105–114. [PubMed: 9254728]
4. Deng X, Liu H, Huang J, et al. Ionizing radiation induces prostate cancer neuroendocrine differentiation through interplay of CREB and ATF2: implications for disease progression. Cancer Res 2008;68:9663–9670. [PubMed: 19047143]
5. Oehler C, Dickinson DJ, Broggini-Tenzer A, et al. Current concepts for the combined treatment modality of ionizing radiation with anticancer agents. Curr Pharm Des 2007;13:519–535. [PubMed: 17348847]
6. Xu L, Yang D, Wang S, et al. (−)-Gossypol enhances response to radiation therapy and results in tumor regression of human prostate cancer. Mol Cancer Ther 2005;4:197–205. [PubMed: 15713891]
7. Dai Y, Liu M, Tang W, et al. Molecularly targeted radiosensitization of human prostate cancer by modulating inhibitor of apoptosis. Clin Cancer Res 2008;14:7701–7710. [PubMed: 19047096]
8. Adams J. The proteasome: a suitable antineoplastic target. Nat Rev Cancer 2004;4:349–360. [PubMed: 15122206]
9. Papandreou CN, Daliani DD, Nix D, et al. Phase I trial of the proteasome inhibitor bortezomib in patients with advanced solid tumors with observations in androgen-independent prostate cancer. J Clin Oncol 2004;22:2108–2121. [PubMed: 15169797]
10. Papandreou CN, Logothetis CJ. Bortezomib as a potential treatment for prostate cancer. Cancer Res 2004;64:5036–5043. [PubMed: 15289299]
11. Sorolla A, Yeramian A, Dolcet X, et al. Effect of proteasome inhibitors on proliferation and apoptosis of human cutaneous melanoma-derived cell lines. Br J Dermatol 2008;158:496–504. [PubMed: 18205878]

12. Yang H, Chen D, Cui QC, et al. Celastrol, a triterpene extracted from the Chinese “Thunder of God Vine,” is a potent proteasome inhibitor and suppresses human prostate cancer growth in nude mice. Cancer Res 2006;66:4758–4765. [PubMed: 16651429]
13. Abbas S, Bhoumik A, Dahl R, et al. Preclinical studies of celastrol and acetyl isogambogic acid in melanoma. Clin Cancer Res 2007;13:6769–6778. [PubMed: 18006779]
14. Wang W, Yang S, Su Y, et al. Enhanced antitumor effect of combined triptolide and ionizing radiation. Clin Cancer Res 2007;13:4891–4899. [PubMed: 17699869]
15. Meng Y, Tang W, Dai Y, et al. Natural BH3 mimetic (−)-gossypol chemosensitizes human prostate cancer via Bcl-xL inhibition accompanied by increase of Puma and Noxa. Mol Cancer Ther 2008;7:2192–2202. [PubMed: 18645028]
16. Feng FY, Lopez CA, Normolle DP, et al. Effect of epidermal growth factor receptor inhibitor class in the treatment of head and neck cancer with concurrent radiochemotherapy in vivo. Clin Cancer Res 2007;13:2512–2518. [PubMed: 17438112]
17. Vallerga AK, Zarling DA, Kinsella TJ. New radiosensitizing regimens, drugs, prodrugs, and candidates. Clin Adv Hematol Oncol 2004;2:793–805. [PubMed: 16166960]
18. Srivastava N, Gochhait S, de Boer P, et al. Role of H2AX in DNA damage response and human cancers. Mutat Res. 2008
19. Banath JP, Macphail SH, Olive PL. Radiation sensitivity, H2AX phosphorylation, and kinetics of repair of DNA strand breaks in irradiated cervical cancer cell lines. Cancer Res 2004;64:7144–7149. [PubMed: 15466212]
20. Paull TT, Rogakou EP, Yamazaki V, et al. A critical role for histone H2AX in recruitment of repair factors to nuclear foci after DNA damage. Curr Biol 2000;10:886–895. [PubMed: 10959836]
21. Ghobrial IM, Witzig TE, Adjei AA. Targeting apoptosis pathways in cancer therapy. CA Cancer J Clin 2005;55:178–194. [PubMed: 15890640]
22. Bonner WM, Redon CE, Dickey JS, et al. GammaH2AX and cancer. Nat Rev Cancer 2008;8:957–967. [PubMed: 19005492]
23. Jacquemont C, Taniguchi T. Proteasome function is required for DNA damage response and fanconi anemia pathway activation. Cancer Res 2007;67:7395–7405. [PubMed: 17671210]
24. Murakawa Y, Sonoda E, Barber LJ, et al. Inhibitors of the proteasome suppress homologous DNA recombination in mammalian cells. Cancer Res 2007;67:8536–8543. [PubMed: 17875693]
25. Krogan NJ, Lam MH, Fillingham J, et al. Proteasome involvement in the repair of DNA double-strand breaks. Mol Cell 2004;16:1027–1034. [PubMed: 15610744]
26. Liu Y, Tseng M, Perdreau SA, et al. Histone H2AX is a mediator of gastrointestinal stromal tumor cell apoptosis following treatment with imatinib mesylate. Cancer Res 2007;67:2685–2692. [PubMed: 17363589]
27. Pawlik TM, Keyomarsi K. Role of cell cycle in mediating sensitivity to radiotherapy. Int J Radiat Oncol Biol Phys 2004;59:928–942. [PubMed: 15234026]
28. Pajonk F, van Ophoven A, Weissenberger C, et al. The proteasome inhibitor MG-132 sensitizes PC-3 prostate cancer cells to ionizing radiation by a DNA-PK-independent mechanism. BMC Cancer 2005;5:76. [PubMed: 16001975]

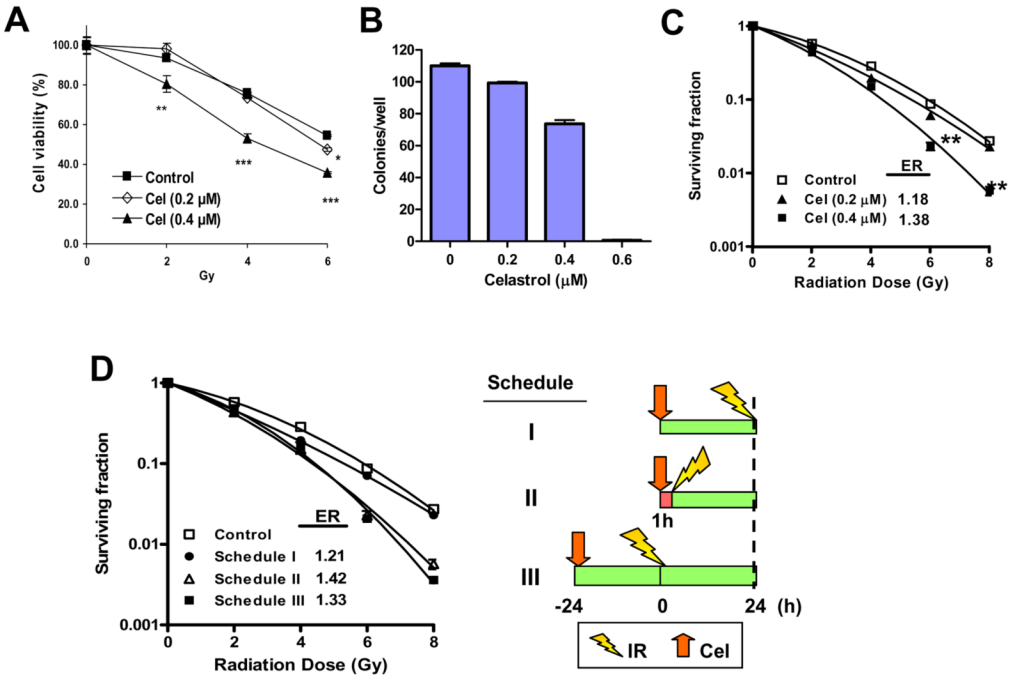

Fig. 1.

Enhanced effect of Celastrol (Cel) with ionizing radiation (IR) on PC-3 cells. ***A***, Cel with IR showed enhanced cytotoxicity. Cells were pre-treated with the indicated concentrations of Cel for 1 h followed by IR. After irradiation, cells were incubated with Cel for 96 h and cell viability was measured. *Bars*, SD (n=3). *p<0.05; **p<0.01; ***p<0.001. ***B***, Cel suppresses cell colony formation. Cells (150 cell/well) were treated with varying concentrations of Cel. Colonies (≥ 50 cells) were counted after 14 days' incubation. *Columns*, mean; *bars*, SD (n=3). ***C***, Cel sensitizes radiation-induced clonogenic cell death. Cells were pre-treated with the indicated concentrations of Cel for 1 h followed by irradiation. After irradiation, cells were incubated with Cel for another 24 h. Cells were then seeded into 6-well plates for clonogenic assay. *Bars*, SD (n=3). **p<0.01. Data represented one of three independent experiments. ***D,*** The schedule-dependence of Celastrol-mediated radiosensitization. *Schedule I*, cells were pretreated with 0.4 μM of Cel for 24 h then irradiated. Right after irradiation, cells were processed for clonogenic survival assay; *Schedule II*, cells were pretreated with 0.4 μM of Cel for 1 h followed by irradiation. After irradiation, cells were incubated with Cel for another 24 h before clonogenic survival assay; *Schedule III*, cells were pretreated with Cel for 24 h then irradiated. After irradiation, cells were incubated with Cel for another 24 h before clonogenic survival assay. *Bars*, SD (n=3). Data represent one of two independent experiments.

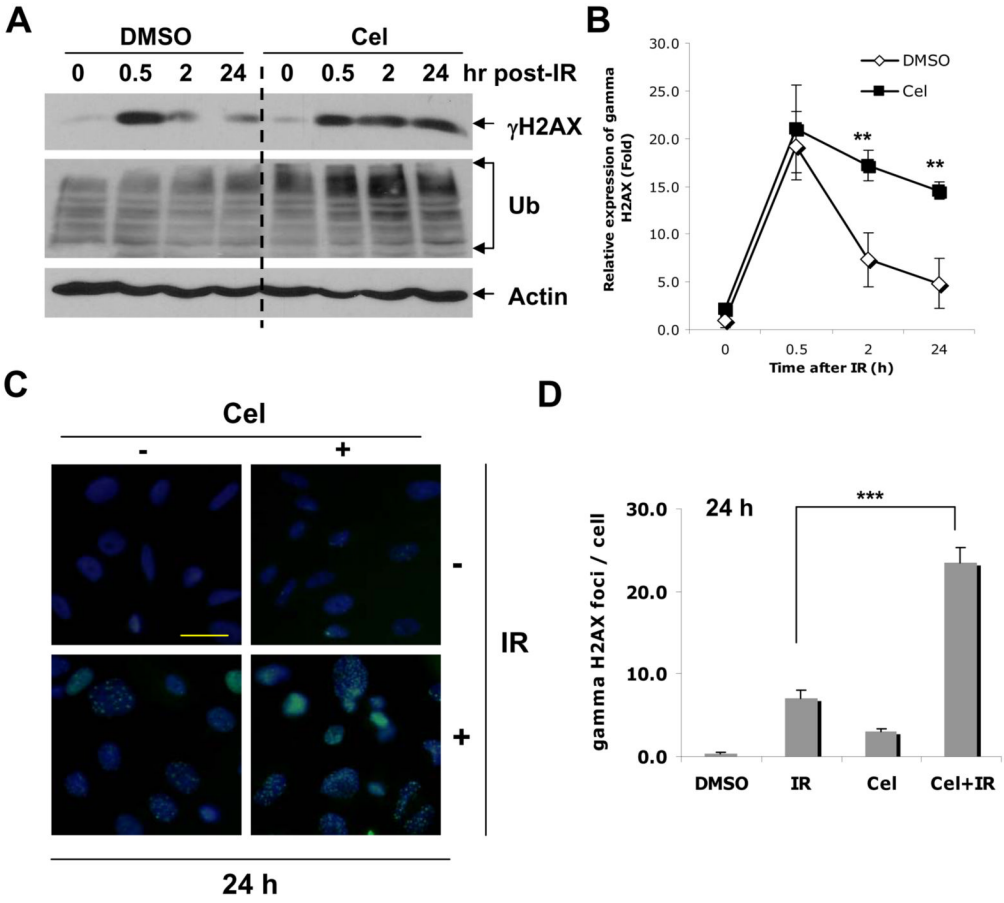

Fig. 2.

Protein expression after treatment with Celastrol and IR. Cells were treated with Cel (0.4 μM) and IR (4 Gy) alone or in combination. For combination treatment, cells were exposed to irradiation and Cel following *Schedule II* in Fig. 1D. ***A***, at desired time points after IR, cells were harvested and whole cell lysates were analyzed by Western blot. ***B***, Relative expression of γH2AX in *A* was expressed by normalizing the ratio of the density to Actin in treated samples with untreated control. ***p*<0.01. *Bars*, SD of two independent experiments. ***C***, Immunostaining of γH2AX by Celastrol and IR. Cells were fixed, permeablized, incubated with anti-γH2AX primary antibody and stained with FITC-labeled anti-mouse secondary antibody. Nuclear γH2AX foci were indicated as green fluorescent dots counterstained with DAPI for nuclear DNA (Original magnification, ×400). ***D***, Quantification of γH2AX foci from *C*. Fifty cells were randomly selected for counting γH2AX foci (Original magnification, ×400). *Columns*, mean; *bars*, SE (*n*=50). ****p*<0.001.

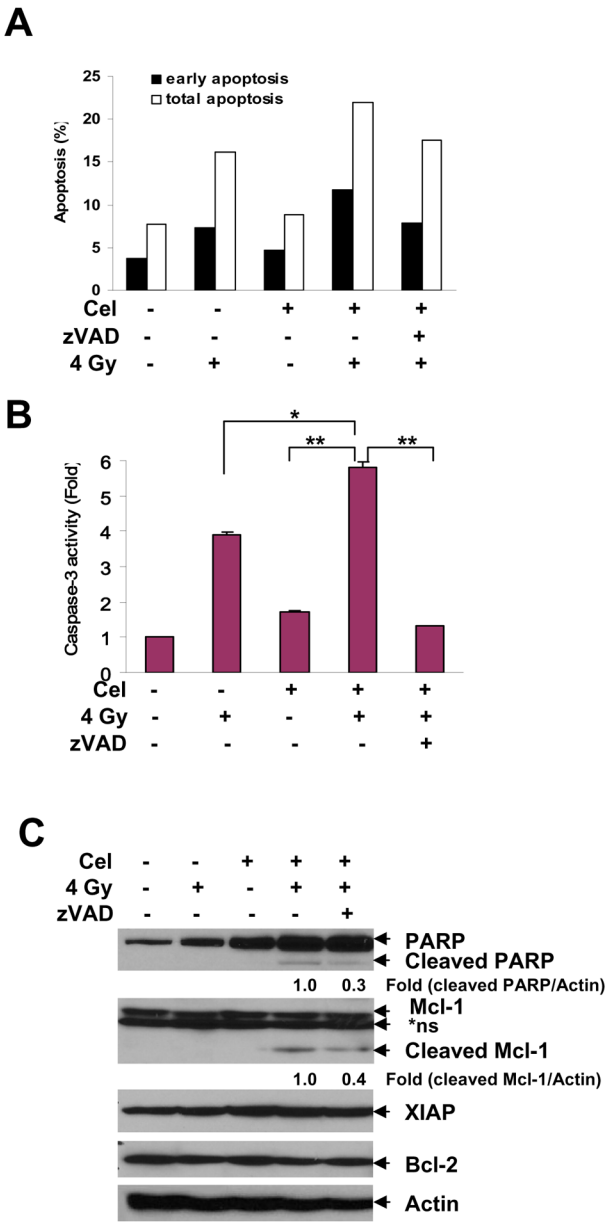

Fig. 3.

Celastrol increased IR-induced apoptosis in PC-3 cells. Cells were treated with Cel (1 μM) and IR (4 Gy) alone or in combination for 72 h, with or without zVAD (2 μM) 1 h pretreatment. For combination treatment, cells were pre-treated with Cel for 1 h and exposed to IR. After irradiation, cells were incubated with Cel for 72 h. ***A***, Cel enhanced IR-induced apoptosis. Cells were harvested and stained by Annexin V-FITC and PI, followed by analysis on flow cytometry. Both early [Annexin(+)/PI(−)] and total [Annexin(+)] apoptotic cell population were counted. Data shown represent one of two independent experiments. ***B***, Cel enhanced IR-induced caspase-3 activation. Cells were lysed and incubate with fluorogenic substrate DEVD-AFC. Proteolytic release of AFC was monitored. Fold increase of fluorescent signal was calculated by dividing the normalized signal in each treated sample by that in the untreated control. *Columns*, mean; *bars*, SD (n=3). *p<0.05; **p<0.01. ***C***, Combination of Cel with IR

triggered PARP and Mcl-1 cleavage. Whole cell lysates (40 μg) were employed for Western blot. Relative expression of cleaved PARP and cleaved Mcl-1 was quantified by normalizing the ratio of the band intensity to Actin in treated samples with untreated control. *ns, non-specific band.

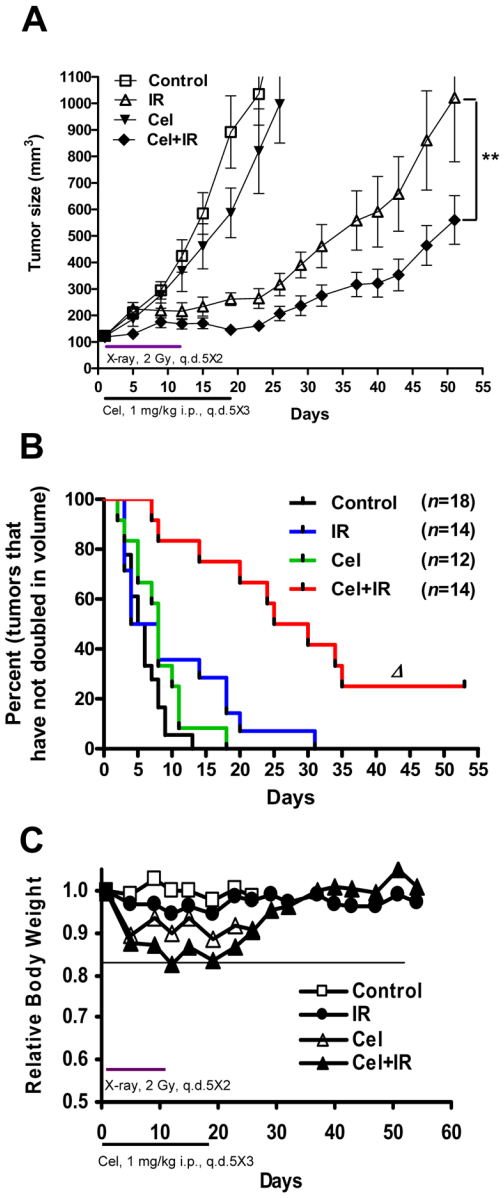

Fig. 4.

Antitumor effect of combination treatment in PC-3 xenografts. ***A***, Nude mice bearing PC-3 tumors were treated as described in *Materials and Methods*. Tumor growth curve was plotted based on average tumor volumes. *Bars*, SE. ***p*<0.01 (two-way ANOVA). ***B,*** Kaplan-Meier curves show the effects of combining Cel with IR on tumor volume doubling time. The median tumor volume doubling time for each group is depicted numerically. Δ, *p*<0.0001 *vs*. IR (Mantel-Cox test). Tumor number (*n*) of each group is shown. ***C***, Relative body weight was calculated by normalizing the average mice body weight in each group (8–10 mice/group) with the weight on the day of initial treatment (day 0).

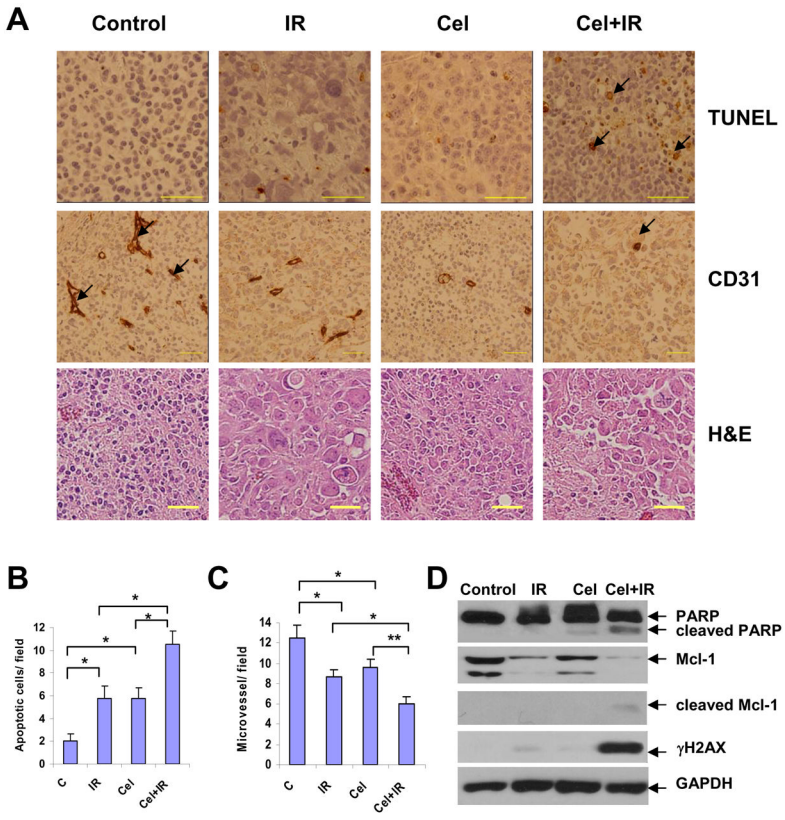

Fig. 5.

Immunohistological analysis and protein expression of tumor tissues. ***A***, tumor sections on Day 18 were embedded in paraffin and processed to H&E, TUNEL, and anti-mouse CD31 immunostaining (original magnification, ×400). In TUNEL assay, the apoptotic cells were positively stained with brown nuclei (indicated by arrows). In CD31 assay, tumor blood vessels were stained brown (indicated by arrows). Both TUNEL-positive tumor cells (***B***) and anti-CD31-positive endothelial cells (***C***) were quantified by randomly counting 8 fields (original magnification, ×200). *Columns*, mean; *bars*, SEM (n=8). *p<0.05; **p<0.01. ***D***, Whole cell lysates (30 μg) of tumor tissues was analyzed by Western blot with respective antibodies.

Table 1

Summary of *in vivo* efficacy

Group	T/C[#] (%)	Tumor doubling time (day)[§]
Control	100.0	5.5 ± 0.7
IR	31.9	6.0 ± 2.3
Cel	71.5	8.0 ± 1.2
Cel+IR	19.0[***]	25.0 ± 3.6[Δ]

[#]NOTE: Tumor growth inhibition (T/C %) was calculated as percentage of the median tumor volume in treatment group divided that in control group, when the control median tumor reached 750 mm^3.

[§]Tumor doubling time was shown as median ± SEM (*n* is shown in Fig. 5B).

[***]*P*<0.001 *vs*. IR (*n*=14);

[Δ]*P*<0.0001 *vs*. IR